Journal of Applied Mathematics and Physics, 2022, 10, 1813-1836
https://www.scirp.org/journal/jamp
ISSN Online: 2327-4379
ISSN Print: 2327-4352

Nuclear Fusion Research and Development Need New Relativistic Mass and Energy Corrections Given by the Information Relativity Theory

Hans Hermann Otto

Materials Science and Crystallography, Clausthal University of Technology, Clausthal-Zellerfeld, Germany
Email: hhermann.otto@web.de

How to cite this paper: Otto, H.H. (2022) Nuclear Fusion Research and Development Need New Relativistic Mass and Energy Corrections Given by the Information Relativity Theory. *Journal of Applied Mathematics and Physics*, **10**, 1813-1836.
https://doi.org/10.4236/jamp.2022.105125

Received: April 12, 2022
Accepted: May 28, 2022
Published: May 31, 2022

Abstract

Hundred years after the conjecture of the British astronomer *Eddington* that the sun is powered by nuclear fusion of hydrogen, new physics theory may help make energy harvesting by nuclear fusion soon a reality. Researchers as well as investors funding fusion megaprojects are asked to deal with new relativistic corrections for mass and energy proposed by *Suleiman* in his Information Relativity Theory (*IRT*). These corrections were calculated in this contribution. It will help to decide whether a venture will be successful and to save big investments when in doubt. The assumed optimal kinetic energy for controlled nuclear fusion must be corrected to a somewhat higher level. At very high kinetic energy in the upper GeV range, it remains not enough baryonic mass to be transformed in energy. The fusion probability faded out to zero already at the golden limit of the recession speed of $v/c = \varphi = \frac{\sqrt{5}-1}{2}$ between target nucleon and projectile nucleon. Cold nuclear fusion, if ever possible, is recommended for protons rather than deuterons at highest experimental possible temperatures around 1000 (K) and needs fine-tuned kinetic nucleon energy. It would be also of interest whether a golden ratio based nuclear fuel confinement chamber could be beneficial. In this connection, also cold nuclear fusion setups should be discussed. Nature is governed by the golden ratio and criticality of physical systems influenced by it, and nuclear physics is not an exception. Computer simulations of the underlying controlled nuclear fusion processes should gain profit from *IRT* corrected starting information and may tackle anew possible low energy nuclear transmutations considering the wave-like dark components of matter and energy.

Keywords

Controlled Thermonuclear Fusion, *IRT* Theory, Relativistic Mass Correction, Low Energy Nuclear Reaction, Golden Ratio, Golden Limit of Nuclear Fusion

1. Introduction

Big ideas often suffer from teething problems caused by the indolence with which just great scientists insist on what they have learnt and worked out. This contribution should serve to support ideas of a new physics and recommends application of these ideas to big projects of the mankind such as thermonuclear fusion research and its technical realization. Success in application of the mentioned theory would also promote the theory itself.

Relativistic mass respectively energy corrections are very important when dealing with nuclear fusion and the dynamics of moving particles, where light atoms combine to larger ones accompanied by conversion of some mass into huge energy. A new theory of *Ramzi Suleiman*, named *Information Relativity* theory (*IRT*), has fixed an overlooked flaw in *Newton's* theory that leads to changes in relativistic corrections [1]. Many formal explanations or physical constructs that bothered long time the world of physics are overcome by the new exciting theory. Recently, the present author has performed relativistic mass corrections on the gyromagnetic factor of the electron [2] that also would change the charge of the electron a little bit [3]. It is connected with the important question whether we need at all the construct of quantization [1] [4]. Ever the golden ratio as the dominate number of nature is involved in such considerations, and so the *IRT* theory has to do with this fundamental number as will be shown below. More than this, the genetic code of the *DNA* is based on a golden mean hierarchy [5]. In this way, it is stringent to deal with the new theory in every area of physics (and of life) knowing that even in fusion science and technology several disciplines of physics are combined. Especially attention must be paid to the wave-like dark component of mass energy density respectively energy density (see **Figure 1**). It is not the intention of the author to keep the reader away from studying the *IRT* theory in detail for himself. Therefore, only a sparse introduction was given. A concise overview on controlled nuclear fusion ideas and different technologies was recently summarized by *Clynes* [6] and should not be explained in detail. This isn't a review article with an almost complete reference list, but a contribution motivating others to think outside the box. In the long run, we have to move away from the large energy projects towards more decentralized producers and distributors for the benefit of our environment.

During the preparation of this contribution, the successful ignition of a controlled thermonuclear fusion reaction maintaining the reaction for about 10 seconds was reported from the staff of the *CFETR* reactor in Hefei, China.

Furthermore, a recent contribution about the creation of elements from nuclear transmutation in Earth lower mantel is highly recommended [7].

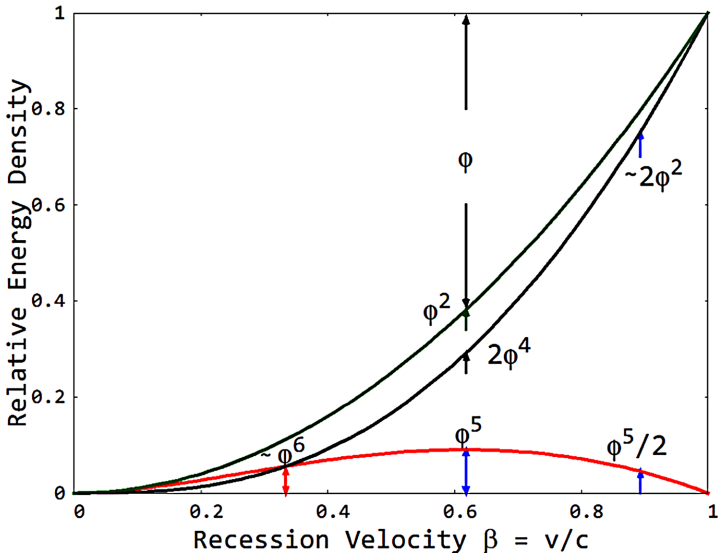

Figure 1. Components of relative energy density versus recession velocity β according to [1]. Red: baryonic matter energy density (Equation (3)), black: dark component (Equation (4)), green: matter energy density sum. The golden mean hierarchy was emphasized [2].

2. New Relativistic Mass and Energy Corrections

Suleiman has set out to correct physical processes for time displacements between observer and moving bodies. Transformations for time duration, length, mass density as well as energy density were applied to a whole bunch of physical phenomena, which could be explained now in simple and beautiful clarity [1]. Indeed, this theory is an outstanding example for the beauty of the simple.

According to the *IRT* theory mass is transformed in dependence of the recession velocity of a moving body as [1]

$$\frac{m}{m_0} = \frac{1-\beta}{1+\beta}. \tag{1}$$

where $\beta = \frac{v}{c}$ is the recession velocity.

For the matter energy density e_M of a moving body with velocity v and rest density ρ_o on yields

$$e_M = \frac{1}{2}\rho v^2 = \frac{1}{2}\rho_o c^2 \frac{1-\beta}{1+\beta}\beta^2 = e_o \frac{1-\beta}{1+\beta}\beta^2, \tag{2}$$

where $e_o = \frac{1}{2}\rho_o c^2$.

The matter energy density reached its maximum at a recession velocity of $\beta = \varphi$, where $\varphi = \frac{\sqrt{5}-1}{2} = 0.6180339887$ is the golden mean. Replacement of this special value in Equation (2) gives

$$\left(e_M\right)_{\max} = e_o \frac{1-\varphi}{1+\varphi}\varphi^2 = e_o\varphi^5 = e_o \cdot 0.09016994\cdots \tag{3}$$

Remembering, φ^5 represents *Hardy*'s maximum quantum entanglement probability [8]. This result was commented by the present author in a publication before mentioned [3].

Suleiman aptly characterized the behavior at the critical point $\beta_{cr} = \varphi$ as phase criticality at cosmic scale [1] [9]. However, φ^5 scaling seems to be a more general quality of phase transitions [10].

The dark matter density transforms as

$$\frac{e_{DM}}{e_o} = \frac{2\beta^3}{1+\beta} \tag{4}$$

If one calculates the energy density amounts (ratios) of matter and dark matter contributions at this point, one gets again a golden mean representation like *Russian* dolls nesting

$$\varphi^3 + 2\varphi^2 = 0.236067976\cdots + 0.763932023\cdots = 1 \tag{5}$$

The difference gives $2\varphi^2 - \varphi^3 \approx \left(\sqrt{2}-1\right)\frac{4}{\pi}$, where $\sqrt{2}-1 = 0.414213\cdots$ is the silver mean. The case, where according to the *Information Relativity* theory of *Suleiman* [1] [9] just at the recession velocity of $ß = 1/3$ the matter and the dark matter density will be the same, delivers for the density amount the reciprocal of *Lucas* number $L_6 = 18$ [2].

The relative energy density components are depicted in **Figure 1** versus the recession velocity *ß*. Also the golden mean hierarchy was displayed.

Instead of the recession velocity it may be useful to choose another variable, the redshift $z = \frac{\beta}{1-\beta}$. Applied matter density transformations in terms of the redshift yield [1]

$$\frac{\rho_M}{\rho_0} = \frac{1}{2z+1} \tag{6}$$

$$\frac{\rho_{DM}}{\rho_0} = \frac{2z}{2z+1} \tag{7}$$

As was demonstrated by Suleiman, an increase of the redshift z caused the matter density of the travelling corpuscular particle successively to diminish, while energy is transformed into the wave-like dark component and vice versa [1]. The complementary duality between matter density and dark matter density versus redshift was illustrated in **Figure 2**.

Both figures describe precisely and elegantly what needs to be considered when dealing with colliding particles of high speed during nuclear fusion, "where each moving particle will be permeated by the dark matter halo of the other one making the two physically entangled" [1].

However, many other scientist have studied the relativity aspect, for instance in the quantum world [11], or in space-time theories preferring the *Selleri* transformation [12].

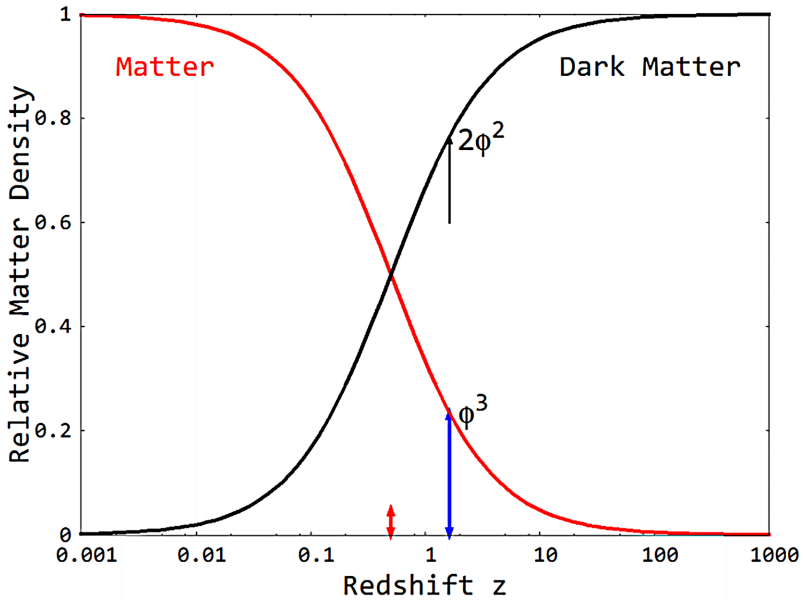

Figure 2. Illustration of the complementary duality between matter density and dark matter density versus redshift. Logarithmic scale, red arrow at $z = 1/2$, blue arrow at $z = \varphi^{-1} = 1 + \varphi = 1.61803398$.

3. Nuclear Fusion Reactions Reexamined

The first researcher who experimentally had demonstrated nuclear fusion was the *Australian* physicist *Oliphant* at Cambridge laboratory in 1934 [13]. The investigated nuclear fusion reactions are the basis of research and development up to now fusing nuclei of hydrogen isotopes deuterium and tritium respectively deuterium and helium-3 according to

$$ {}_1^2\mathrm{D} + {}_1^3\mathrm{T} \rightarrow {}_2^4\mathrm{He} + {}_0^1\mathrm{n} + 17.6\ \mathrm{MeV} \tag{8} $$

$$ {}_1^2\mathrm{D} + {}_2^3\mathrm{He} \rightarrow {}_2^4\mathrm{He} + {}_1^1\mathrm{H} + 18.4\ \mathrm{MeV} \tag{9} $$

The stability of atomic nuclei can be found in textbooks of nuclear physics, where the average binding energy per nucleon is depicted versus the atomic mass number (**Appendix** Figure A1).

The energy gain according to the basic exothermic fusion reaction (8), for instance, can be calculated from the difference in the rest energy of the constituents given in MeV

$$ Q = (1875.6129 + 2809.4318 - 3728.3995 - 939.5653)\,\mathrm{MeV} = 17.59\ \mathrm{MeV} \tag{10} $$

whereas deuterium is abundantly available in seawater coming from comets that have reached the earth, for tritium there exists no sizable natural source due to its radioactive decomposition within a half-life time of about 12.3 years.

Tritium must therefore be produced by breeding from lithium [14], for instance by its reaction with neutrons produced during the fusion processes (tritium self-sufficiency).

In the near future, mankind will be able to extract by extraterrestrial mining ${}_2^3\mathrm{He}$ from the sunlit areas of the moon as a third-generation fusion fuel. This

stable isotope stems from solar wind and has been stored in moon's uppermost rock layers. A possible fusion reaction between these nucleons is

$$^{3}_{2}\mathrm{He} + {}^{3}_{2}\mathrm{He} \rightarrow {}^{4}_{2}\mathrm{He} + 2\,{}^{1}_{1}\mathrm{p}^{+} + 12.86\ \mathrm{MeV} \tag{10}$$

An assumed cold nuclear fusion reaction, for instance, starting with two deuterons confined in an interstitial of the palladium metal lattice, would result in

$$^{2}_{1}\mathrm{D} + {}^{2}_{1}\mathrm{D} \rightarrow {}^{4}_{2}\mathrm{He} + 23.85\ \mathrm{MeV} \tag{11}$$

The binding energy of the nucleons in the deuteron is relatively small and about 2.2 MeV. The nucleons (proton and neutron) are relatively far apart from each other by about 4 fm. Therefore, also a cascade of the following energetically more favorable reactions should be considered with three deuterons involved temporarily

$$^{2}_{1}\mathrm{D} + {}^{2}_{1}\mathrm{D} \rightarrow {}^{3}_{2}\mathrm{He} + {}^{1}_{0}\mathrm{n} + 3.27\ \mathrm{MeV} \tag{12}$$

$$^{2}_{1}\mathrm{D} + {}^{3}_{2}\mathrm{He} \rightarrow {}^{4}_{2}\mathrm{He} + {}^{1}_{1}\mathrm{p}^{+} + 18.87\ \mathrm{MeV} \tag{13}$$

$$^{1}_{0}\mathrm{n} + {}^{1}_{1}\mathrm{p}^{+} = {}^{2}_{1}\mathrm{D} + 1.71\ \mathrm{MeV} \tag{14}$$

Byproducts such as neutrons or sometimes tritium when excess of deuterium reacts with neutrons have been reported as observed experimentally [15]. A summing up of these reactions delivers again reaction (11). One can indeed place three neighboring deuterons in an octahedral interstitial of palladium besides nearby tetrahedral ones. In contrast to bulk PdD_x, where only octahedral sites are occupied, in the subsurface region of nanometer-sized material of PdH_x, also 30 percent of tetrahedral sites are occupied besides 70 percent of octahedral ones [16]. The same occupation scheme may be assumed for isomorphic PdD_x. For cold fusion experiments, a high deuterium loading near the ratio Pd/D = 1 is of interest [17].

Now we want to set up the equation of motion for the colliding particles keeping a fuel of heavy water and lithium in the plasma state and accelerate deuterons towards the target. At very high particle speed we have to consider duality between both particles and waves (dark matter surrounding) using an elastic atomic collisions model as well as an elastic spring model associating the atomic collision model with particles and the spring model with waves. With respect to the speed probability distribution during a two-body collision between particles one can apply the *Lattice Boltzmann Method* (*LBM*) as a combination of the *Boltzmann* equation and the *Maxwell-Boltzmann* distribution function [18].

The tunneling probability P_G of two nuclear particles to overcome the *Coulomb* barrier was derived by *Gamov* [19] being

$$P_G(E) = \exp\left(-\sqrt{\frac{E_G}{E}}\right) \tag{15}$$

The *Gamov* energy E_G resulted in

$$E_G = \left(\pi\alpha Z_A Z_B\right)^2 2\mu c^2 \tag{16}$$

and the kinetic energy is

$$E = \frac{1}{2}\mu v^2 \tag{17}$$

where α is *Sommerfeld*'s fine-structure constant, μ is the reduced mass, v is the speed between the two particles, c is the speed of light, and Z_A respectively Z_B are the proton numbers of the nucleons A respectively B. Importantly, the fine-structure constant α in relation (16) has to be changed marginally [2] [3].

Using the *IRT* transformation for mass according to relation (1), the reduced mass μ for a reaction involving two equal nuclear particles of rest mass m_0 gets

$$\mu = \frac{m_0}{2} \cdot \frac{1-\beta}{1+\beta} \tag{18}$$

Finally one gets together with Equation (2)

$$P_G(E) = \exp\left(-2\pi\alpha Z_A Z_B/\beta\right) \tag{19}$$

Following now *Cooley* [20] and considering that the particle's speed v is distributed by a *Maxwell-Boltzmann* function one can finally verify the probability (reactivity) for a fusion reaction to occur with two opposing energy terms under the exponential function

$$\langle\sigma v\rangle = \left(\frac{8}{\pi\mu}\right)^{1/2} \cdot \frac{S_0}{(kT)^{\frac{3}{2}}} \cdot \int_0^\infty \exp\left[-\left(\frac{E}{kT} + \sqrt{E_G/E}\right)\right] \mathrm{d}E \tag{20}$$

where σ is the nuclear cross section expressing the likelihood of interaction between projectile particle and target

$$\sigma_{AB}(E) = \frac{S_0}{E} P_G(E) \tag{21}$$

The *Maxwell* averaged fusion cross section $\langle\sigma v\rangle$ or reactivity has the dimension of $\mathrm{cm^2 \cdot cm/s} = \mathrm{cm^3/s}$ with a constant S_0 ($\mathrm{cm^2 keV}$). It should be noticed that the upper integration limit of ∞ in relation (20) is likely to be problematic because the speed of light is considered as limited. Therefore, Equation (23) in the following explanation represents a more concise form using $\beta = v/c$ instead of v.

The maximum of the non-relativistic integrant of relation (20) can be found by setting the first derivative equal to zero [20]

$$E_{\max} = \left(\frac{kT}{2}\right)^{2/3} E_G^{1/3} \tag{22}$$

giving

$$\beta_{\max} = 2\sqrt{\frac{E_{\max}}{e_D}} = \sqrt[3]{4} \cdot \frac{(kT)^{\frac{1}{3}} E_G^{\frac{1}{6}}}{\sqrt{e_D}} = \sqrt[3]{4} \cdot \left(\frac{kT}{e_D}\right)^{1/3} \cdot \left(\frac{E_G}{e_D}\right)^{1/6} \tag{23}$$

Inserting relation (22) in Equation (20) results in

$$\langle\sigma v\rangle_{\max} = \left(\frac{8}{\pi\mu}\right)^{1/2} \cdot \frac{S_0}{(kT)^{3/2}} \cdot \exp\left(-3\left(\frac{E_G}{4kT}\right)^{1/3}\right) \tag{24}$$

Approximating Equation (20) by a *Gaussian*, one can calculate the integral width w_i yielding

$$w_i = \frac{2\sqrt{\pi}}{\sqrt{3}} kT \left(\frac{E_G}{4kT}\right)^{1/6} \tag{25}$$

and then the integral content

$$\langle \sigma v \rangle_{\max} \cdot w_i = \frac{4\sqrt{2}}{\sqrt{3}} \frac{S_0}{\sqrt{kT} \cdot \sqrt{\mu}} \cdot \left(\frac{E_G}{4kT}\right)^{1/6} \cdot \exp\left(-3\left(\frac{E_G}{4kT}\right)^{1/3}\right) \tag{26}$$

The approximation by a *Gaussian* is compared in Figure 3 for the case of proton fusion applying kT = 1 keV. A better adaption between both curves would result when the maximum of the *Gaussian* would be shifted to somewhat higher values > 4.98 keV (for example see right side of Figure 3).

In Table A1 of the Appendix $\beta_{\max}$ values for selected kT have been compared for the non-relativistic case and the *IRT* corrected case. In Figure 4, the tunneling probabilities and $E_{\max}$ values at kT = 1 keV for proton and deuteron nuclei have been compared. Notice the significantly higher proton probability increased by a factor of about 68.5 compared to deuterium.

The representation of the fusion probability in relation to the kinetic energy can be done also in logarithmic form as performed in Figure 4 because $\beta \propto \sqrt{E_{kin}}$ to compare both ß representation and kinetic energy one. If one would translate the given result in the parlance of cold fusion it seems to be evident that proton fusion should be happen much more likely than deuterium fusion, if possible at all.

The *Information Relativity* theoretical solution based on Equation (20) yielded the fusion probability in relation to the recession velocity β indirectly involving the golden mean, where $\langle \sigma\beta \rangle$ has the dimension of (cm²) and e_D = 1875.61294257(57) (MeV) represents the rest energy of the deuteron [21] [22]. Integration is now taken within the changed limits from β = 0 to 1

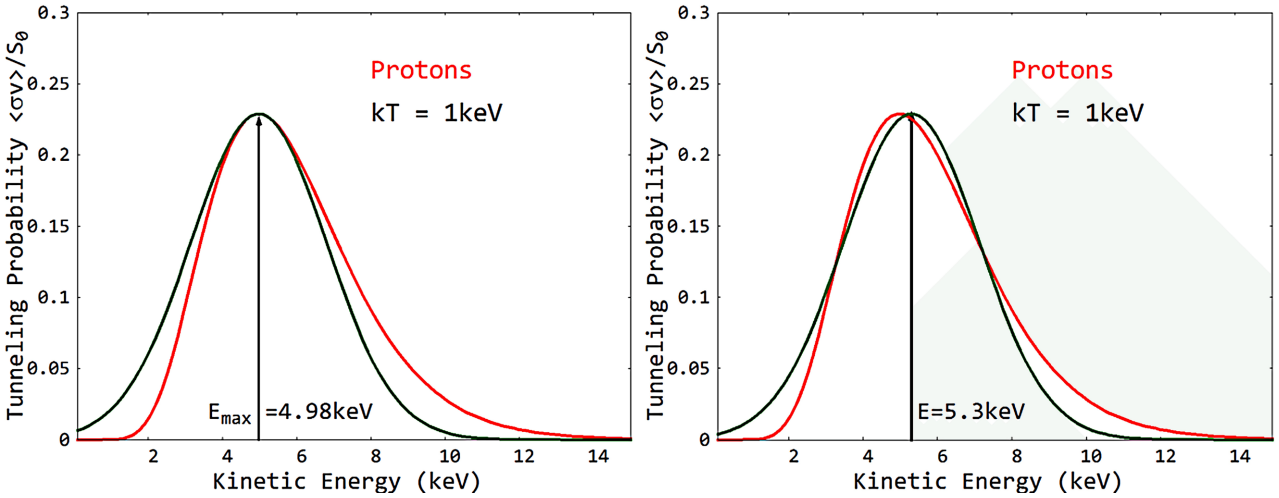

Figure 3. Left: Comparison of the asymmetric fusion probability for protons (red) with a *Gaussian* (green) using maximum and integral width according to Equations (24) respectively (25). Right: Shift of the *Gaussian* showing for instance its maximum now at 5.3 keV.

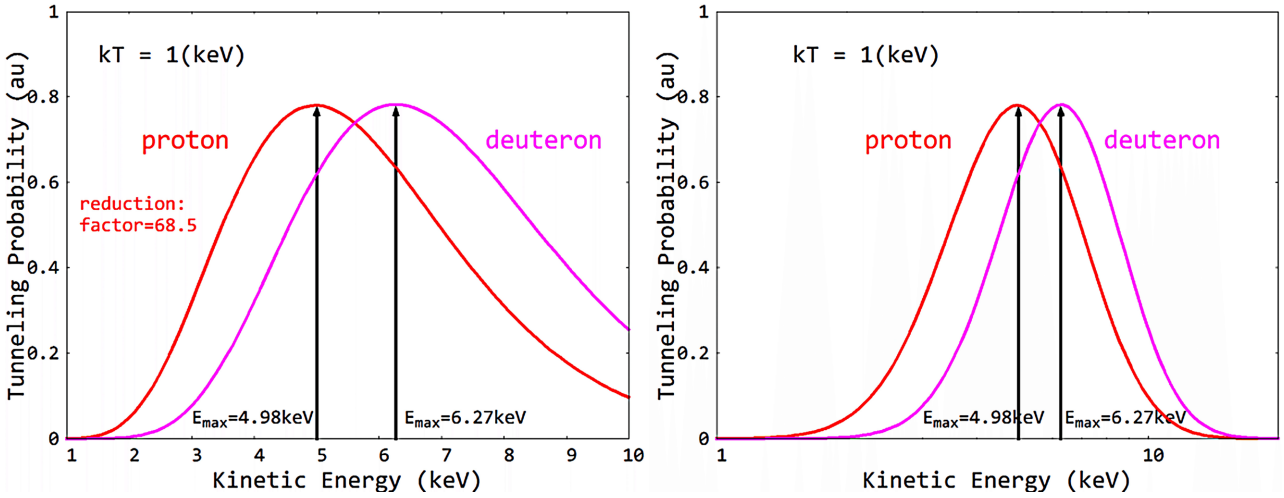

Figure 4. Tunneling probability (arbitrary units) versus kinetic energy for non-relativistic proton respectively deuteron fusion at $kT = 1$ keV. The right figure used a logarithmic scale.

$$\begin{aligned}\langle\sigma\beta\rangle &= \frac{1}{c}\left(\frac{8\cdot 2(1+\beta)}{\pi m_D(1-\beta)}\right)^{1/2}\cdot\frac{S_0}{(kT)^{\frac{3}{2}}}\cdot\int_0^1\exp\left(-\frac{e_D}{4kT}\frac{1-\beta}{1+\beta}\beta^2-\frac{2\pi\alpha Z_A Z_B}{\beta}\right)\\ &\quad\cdot\frac{e_D\cdot\beta(1-\beta-\beta^2)}{2(1+\beta)^2}\mathrm{d}\beta\\ &= \frac{2}{\sqrt{\pi}}\cdot\left(\frac{e_D}{kT}\right)^{1/2}\frac{S_0}{kT}\cdot\int_0^1\frac{\beta(1-\beta-\beta^2)}{(1+\beta)\sqrt{1-\beta^2}}\\ &\quad\cdot\exp\left(-\frac{e_D}{4kT}\frac{1-\beta}{1+\beta}\beta^2-\frac{2\pi\alpha Z_A Z_B}{\beta}\right)\mathrm{d}\beta\end{aligned}\tag{27}$$

The first integrand term being solely a function of β has a maximum of $f(\beta)=0.147847\approx\varphi^4=0.145898\cdots$ at a recession speed of $\beta_{\max}=0.314026\approx 0.30901699=\varphi/2$ (see **Appendix**). It means that the maximum relative particle speed should be about a third of that of light. When following the blue outlined curve in Figure 5, this parabola-like function has zeros at $\beta=0$ respectively $\beta=\varphi$, but is not fully symmetrical, when mirrored at a vertical through $\beta=\varphi/2$. Because we are dealing with a polynomial of third degree, a third physically not meaningful zero is found at $\beta=-\varphi^{-1}$. This pre-factor is responsible for fading out of the tunneling probability of nuclear fusion to zero at the golden mean limit $\beta=\varphi$, just at the recession speed, where the relative energy density of baryonic matter reaches its maximum. Once more this golden limit can be assigned as a phase critical point transforming matter and energy [1] [2].

The tunneling probability was calculated for the case of colliding deuterons depending of the recession speed as well as in dependence to the kinetic energy. The result was depicted in Figure 6 for the case of $kT = 1$ keV. The $E_{\max} = 6.61$ keV value is slightly larger than that for the non-relativistic case with $E_{\max} = 6.27$ keV. Also the half-width of the curve is pronounced greater using the *IRT* approach.

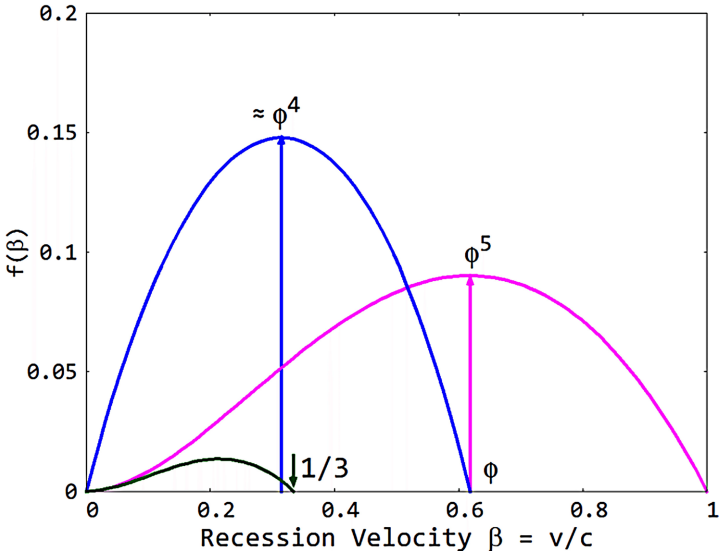

Figure 5. A comparison of different functions of the recession velocity $\beta = \frac{v}{c}$. Magenta: *Hardy*'s quantum probability function respectively *Suleiman*'s energy density according to Equation (2) with the maximum of φ^5 at $\beta = \varphi$. Green: Difference curve between energy density and dark energy density. Blue: Parabola-like curve given by the first integrand term of Equation (27).

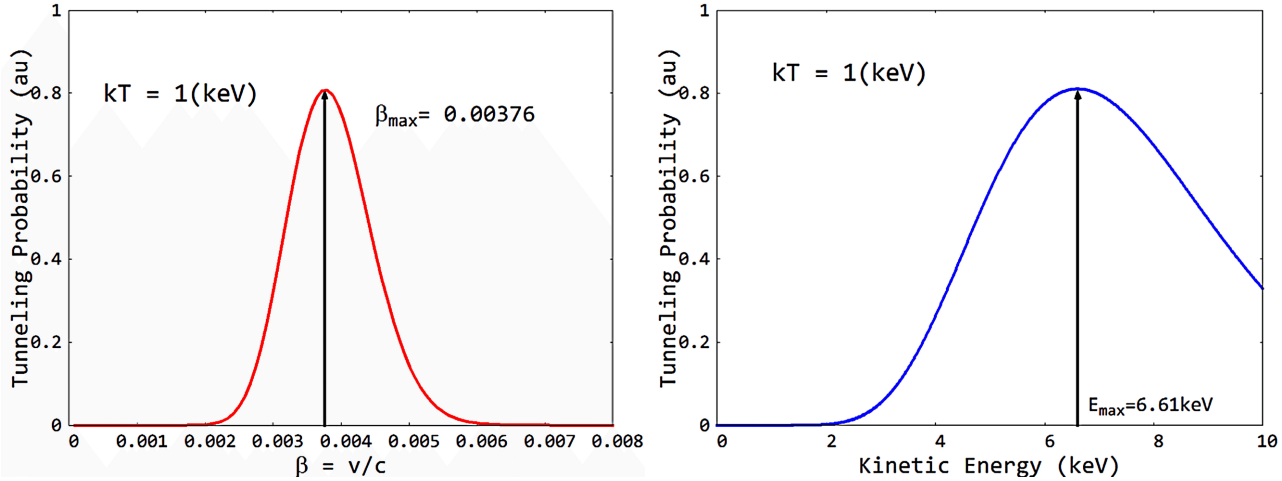

Figure 6. Tunneling probability (arbitrary units) for deuterons with $kT = 1$ keV. Left: versus recession velocity, right: versus kinetic energy (compare **Figure 4**).

The β representation is better suited to be approximated by a *Gaussian*. One can further ask at which kT the maximal probability is realized. This can be done by calculating $\frac{\mathrm{d}\langle\sigma\beta\rangle}{\mathrm{d}(kT)} = 0$. Its solution yielded

$$(kT)_{\max} = \frac{1}{6} e_D \frac{1-\beta}{1+\beta} \beta^2 \tag{28}$$

for $\beta = \beta_{\max}$. Inserting this result into Equation (27) leads to the following simplified expression for maximum kT

$$(kT)_{\max} : \langle \sigma\beta \rangle_{\max} = 12 \cdot \sqrt{\frac{6}{\pi}} \cdot \exp\left(-\frac{3}{2}\right) \frac{S_0}{e_D} \cdot \frac{1-\beta-\beta^2}{\beta^2 (1-\beta)^2} \exp\left(-\frac{2\pi\alpha Z_A Z_B}{\beta}\right) \quad (29)$$

Figure 7 depicts a set of curves for different kT values indicating the overall maximum for kT = 160.4 keV at $ß_{\max}$ = 0.023188 (E_{kin}= 240.7 keV) according to Equation (26). Covering all maxima with an envelope shows that the limiting value is $ß = 1/3$, where the probability at very high kT faded out to become completely zero. According to IRT at this special recession speed the amounts of matter density and dark matter density will be equal (Figure 1) [1] [2].

We will not write down the complex eighth degree polynomial resulting as first derivative of Equation (27) to determine the zeros and maxima of that function, but instead use an approximation by modifying the simpler non-relativistic result given in Equation (23). Whereas the low-kT data follow the non-relativistic result, the high-kT data can be approximated by a relation having the golden mean φ in its pre-factor and exponent

$$\beta_{\max}(kT) \approx \frac{\sqrt[3]{4}}{\varphi^3} \cdot \left(\frac{kT}{e_D}\right)^{\varphi/\sqrt{2}} \cdot \left(\frac{E_G}{e_D}\right)^{\varphi/2\sqrt{2}} \approx \frac{\sqrt[3]{4}}{2\varphi} \cdot \left(\frac{kT}{e_D}\right)^{\varphi/\sqrt{2}} \quad (30)$$

Another simple approximation valid over a larger kT range is given by the relation

$$\beta_{\max}(kT) \approx \exp\left(\frac{3}{4}\sqrt{2} \cdot \left(\frac{kT}{e_D}\right)^{\sqrt{2}-1}\right) - 0.9993 \quad (31)$$

The different relationships were double-logarithmically documented by Figure 8.

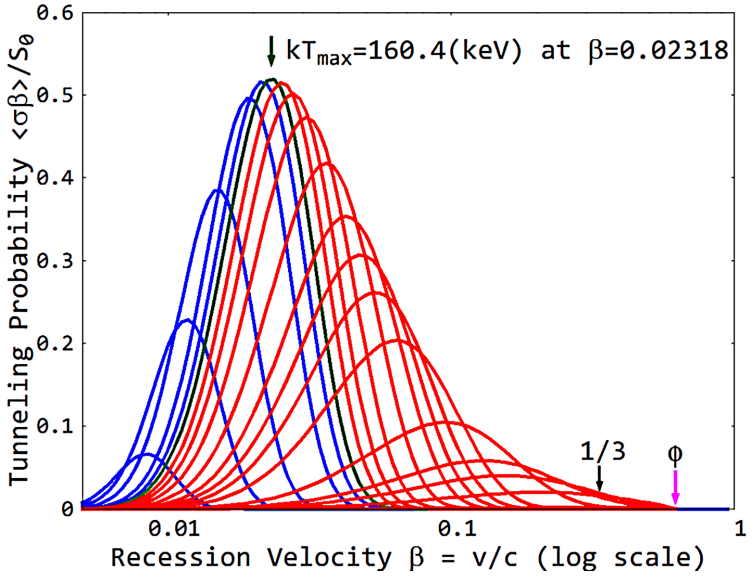

Figure 7. Deuteron tunneling probability for a set of kT values (recession speed logarithmic scaled). The green arrow marks the green outlined maximum curve for kT = 160.4 (keV) at $ß = 0.02319$, and the magenta arrow depicts the ultimate zero probability at limiting $\beta = \varphi = 0.6180339887$.

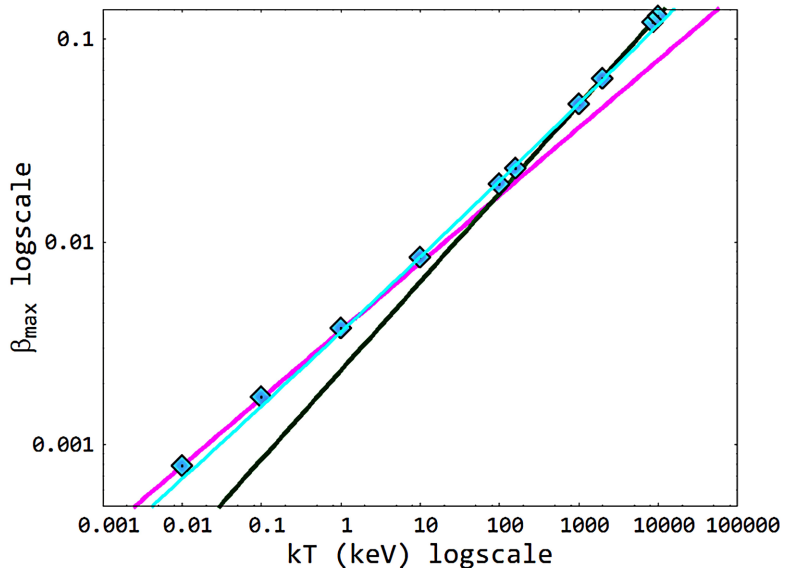

Figure 8. Double logarithmic representation of kT versus the corresponding $\beta_{\max}$ for deuteron fusion. Magenta straight line: non-relativistic case according to Equation (23). Green straight line: linear approximation of the high-kT relativistic data. Cyan curve: approximation according to relation (31).

However, the reader may find a more appropriate approximation for relation (27) using Taylor series development [23] [24].

In addition, on can verify that at maximum kT it holds

$$\frac{E_{kin}}{kT_{\max}} = \frac{3}{2} \tag{32}$$

as well as [25]

$$\beta_{\max} \approx \pi\alpha Z_A Z_B = 0.022935 Z_A Z_B \approx \frac{6\alpha}{5\varphi^2} Z_A Z_B \tag{33}$$

Again it should be pointed out that according to the *IRT* theory the charge of the electron respectively *Sommerfeld*'s fine-structure constant have to be marginally but in view of the given high accuracy still noticeably corrected [2].

In this contribution arbitrary unit for the fusion probability were used because some parameters such as the slightly energy-dependent (astrophysical) parameter S_0 are not sufficiently correct known and should be verified by a modified model calculation (see Equation (21) and (23)).

A more quantitative prediction of the released power ε per unit mass and per second (power density) follows a non-relativistic approach already given by *Cooley* [20], but in an altered form and exemplified for protons

$$\epsilon = \frac{2^{8/3}}{\sqrt{3}} \cdot \frac{c \cdot \rho \cdot X_A X_B}{m_H^2 A_A A_B \sqrt{e_P}} Q S_0 \frac{E_G^{1/6}}{(kT)^{2/3}} \exp\left[-3\left(\frac{E_G}{4kT}\right)^{1/3}\right] \tag{34}$$

where X_A respectively X_B are the nucleon abundances, ρ is the mass density, A_i are the atomic numbers, c is the speed of light, and $S_0 = 4\times10^{-46}\ \mathrm{cm}^2 \cdot \mathrm{keV}$. The proton fusion reaction [18]

$$\mathrm{p}+\mathrm{p}\rightarrow \mathrm{d}+\mathrm{e}^{+}+\upsilon_{\mathrm{e}} \tag{35}$$

delivers an energy of

$$Q = 26.74\ \mathrm{MeV} - 0.52\ \mathrm{MeV} = 26.2\ \mathrm{MeV} \tag{36}$$

when identical nucleons collide, $X_A = X_B = 0.5$, the collision rate has in addition to be divided by 2. For conditions at the core of the sun (kT = 1 (keV), ρ = 150 g·cm^{-3}) one can use the small energy unit of 1 (erg) = 10^{-7} (J) and calculate the non-relativistic power density to be about

$$\epsilon_{\text{sun core}} \approx 11.8\ \mathrm{erg}\cdot\mathrm{g}^{-1}\cdot\mathrm{s}^{-1} \tag{37}$$

Turning now to the relativistic relation (24) and approximate the *Gaussian*-like fusion probability integral by the area given by multiplication of the height $\langle\sigma\beta\rangle_{\max}$ with the integral width $w_i = \dfrac{\sqrt{\pi}}{2\sqrt{\ln(2)}}\cdot w_{FW}$ giving [26]

$$\langle\sigma\beta\rangle / S_0 = \frac{\sqrt{\pi}}{2\sqrt{\ln(2)}}\langle\sigma\beta\rangle_{\max}\cdot w_{FW} \tag{38}$$

Again, with proton abundances $X_A = X_B = 0.5$ and atomic number $A_A = A_B = 1$ one finally yields for the relativistic power density

$$\varepsilon^{*} = \frac{1}{2}\frac{\sqrt{\pi}}{2\sqrt{\ln(2)}}\frac{c\cdot\rho\cdot X_A X_B}{m_H^2 A_A A_B\sqrt{e_P}}\cdot Q\cdot S_0\cdot\langle\sigma\beta\rangle_{\max}\cdot w_{FW} \tag{39}$$

For kT = 1 keV one can estimate $\langle\sigma\beta\rangle_{\max} = 0.001748$ respectively $w_{FW} = 0.002039$ giving

$$\varepsilon^{*}_{\text{sun core}} \approx 13.2\ \mathrm{erg}\cdot\mathrm{g}^{-1}\cdot\mathrm{s}^{-1} \tag{40}$$

Specialists in the field of controlled thermo-nuclear fusion can use own experimental values such as the chosen kT and mass density of the nuclear fuel to verify result obtained with relation (39) using the different concepts of low fuel density combined with extreme temperature contrary to high fuel density and less temperature.

If one briefly summarizes the main results, the following can be noted. There exists a natural golden limit, where nuclear fusion stops down to zero probability. This happened at the recession speed between nucleons of $\beta = \varphi$. The probability distribution curve as a function of the nucleon speed is pronounced broader than in the case of the non-relativistic approach. The maximum probability is found at markedly enhanced speed respectively kinetic energy (see right side of Figure 5). In the GeV range of kT the maximum probability is found at $\beta = \dfrac{1}{3}$, straight at the recession speed at which baryonic matter energy and dark matter energy will become equal. It simply means the more moving matter is transformed to its wave-like dark component, the less is available to be transformed in released energy by fusion of nucleons.

In the range of high particle speed hot fusion takes place in the halo of surrounding dark matter energy emerging from moving particles. It should be con-

sidered in an adequate way by varying Equation (23). A related correction is in progress. Recently, such matter—dark matter coupling was excellently described for the case of disk galaxies by *Suleiman* [27]. Besides the action or involvement of dark matter in fusion physics also the validity of the *Gamov* approach [19] should be questioned critically.

Last but not least the probability for cold fusion remains an open question. Some *IRT* based calculations are summarized in the following chapter.

4. Cold Nuclear Fusion or Transmutation

For the cold fusion at low kT a very sharp energy distribution around the cross section probability maximum can be expected. A cold fusion experiment must optimally meet these requirements for maximum kinetic energy in order to be successful at all. In the following calculated fusion probability curves for deuterium respectively proton nuclei are shown. In **Figure 8** the probability for deuteron fusion within the low-temperature range between 10^3 K and 10^5 K was presented depicting their small *Gaussian*-like distribution curves (T instead of kT was used). However, a further reduction of temperature failed to process the needed number of decimals with a home PC.

For the proton fusion the probability is markedly enhanced compared to deuterium fusion, and so the 500 K values could be calculated, too. If ever cold fusion is detectable, it should be realized using hydrogen at the experimentally highest possible temperature, for instance choosing about 1000 K = 727˚C, for which the result is depicted in **Figure 9**. For $T = 1000$ K one yields $\beta_{\max} = 0.20375$ corresponding to $v_{\max\max} \approx 60(\mathrm{km/s})$ as the optimum speed with which the nuclei should be moved towards each other. The full width at half maximum is about $\Delta\beta_{\max} = 1.84\times10^{-5}$ (**Figure 9**). See also **Table A1** in the **Appendix**.

The draft of a more quantitative picture is currently under progress. In advance some ideas will be presented in the next chapter (**Figure 10**).

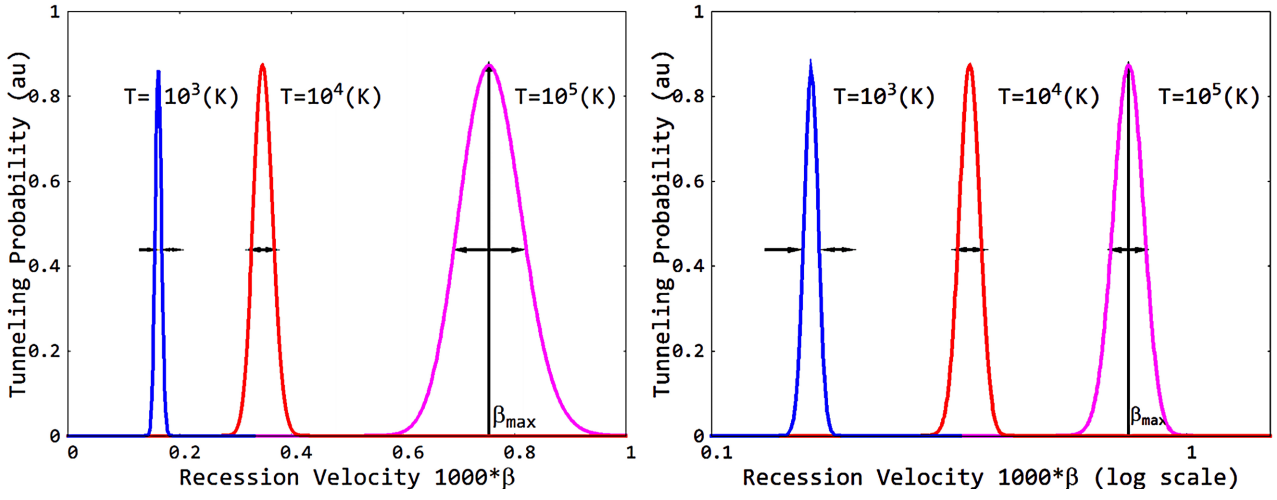

Figure 9. Tunneling probability for deuterons within the low-temperature range (10^3 K to 10^5 K) indicating the extremely different half-width of the curves. The three curves of very different maxima have been adapted all to an equal height.

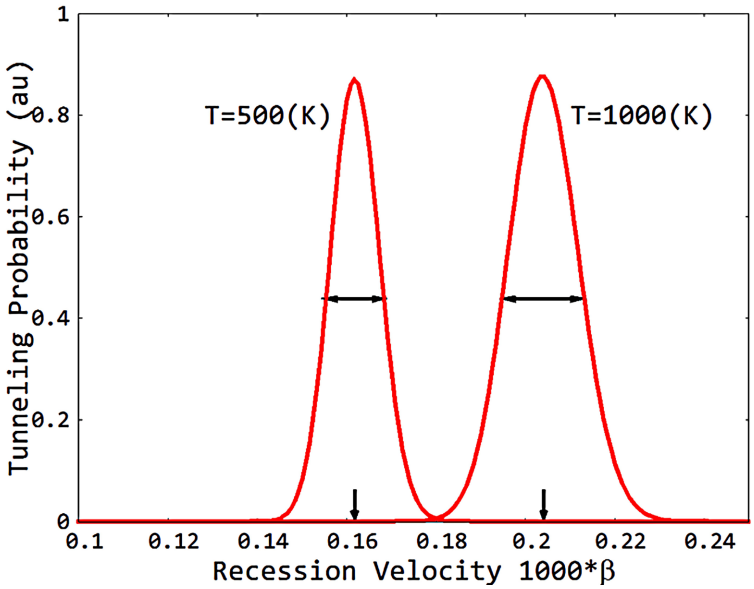

Figure 10. Widths of fusion probability curves for protons at "low" temperatures. The 500 K curve must be reduced by a tremendously large factor of about 3×10^{34} in comparison to the 1000 K one (**Table A2**).

5. Tesla's Energetic Pyramid Conjecture and Beyond

In connection with the Great Pyramid, mention may be made of the vision of the great inventor *Nicola Tesla* to harvest free energy from what we now characterize as dark components of matter respectively energy. Intuitive knowledge of great thinkers shouldn't be confused with obsession. The reader can find more information about this discussion in the references [28] and [29]. Be that as it may, the golden mean based architecture of the Great Pyramid can serve as a proposal for a quite asymmetric nuclear fuel confinement chamber. In this connection the reader may also study the in-ellipsoid approach for less-symmetric solids such as the Great Pyramid to stimulate new ideas [30]. **Figure 11** shows a sketch of two opposed deuterium nucleons in an asymmetric-pyramidal micro-cage waiting for cold fusion to helium according to reaction (11), where the Great Pyramid served as a model.

Cold fusion experiments were described with atomic deuterium occluded in the cubic face-centered palladium lattice having 4 octahedral interstitials besides 8 tetrahedral ones in the unit-cell. First evidenced by *Fleischmann and Pons* [31], the reader may follow an explanation of lattice assisted low-energy nuclear fusion recently given by *Garai* [32], where two protons respectively deuterons are confined in the octahedral interstitials of the cubic Pd lattice. Theoretical considerations of *Gurbich* [33] indicate the problem of cold fusion.

Now we turn back to a pyramidal environment in contrast to the octahedral hole within the Pd lattice. If one would deposit Pd on the surface of a thin mica sheet and bend it cylindrically, the half-octahedral interstitial would be deformed towards the case described in **Figure 9**.

Possibly the occluded deuterons would be asymmetrically positioned at the

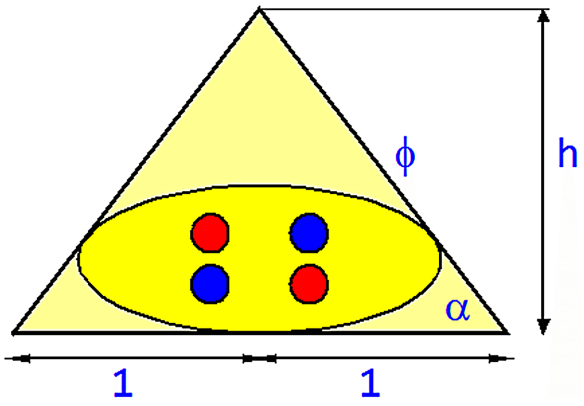

Figure 11. Design of a pyramidal micro-cage containing two opposed deuterons consisting of proton (red) and neutron (blue). The yellow area is the projected maximum in-ellipsoid of such pyramid, where big $\phi = \frac{1+\sqrt{5}}{2} = 1+\varphi$ and $\alpha = \arctan\left(\sqrt{\phi}\right) = 51.82729^\circ$ [27] [28].

interface between mica and palladium as illustrated in **Figure 11**. It is suggested that a fusion reaction could be enhanced by such lattice deformation. However, we are still seeking for a more suitable host material. For micro-scale reactors one could deposit palladium on an atomic flat and highly reflecting (111) gold platelet [34] where the gold substrate serves also as a diffusion barrier for hydrogen or deuterium [35]. The PdH_x respectively PdD_x contact layer is strained due to mismatch between the lattice parameters of gold and PdH_x (PdD_x) and should be able to host even more hydrogen or deuterium in the widened lattice. The upload of deuterium into the Pd lattice was estimated to be about 1.2×10^{23} cm^{-3} [36]. Then one can calculate the mass density yielding $\rho \approx 0.8\ g \cdot cm^{-3}$.

The movement of the two nucleons against each other starting a fusion reaction can be supported by chaotic excessive resonance caused by focused ultrasonic energy loading of the confinement lattice bouncing back the nucleons from the walls with extremely high speed overcoming their *Coulomb* barriers [37] [38] [39] [40]. Fine-tuning of the applied cavitation energy according to the fusion probability maxima given in Chapter 4 is recommended. It is assumed that golden ratio governed geometry of the confinement can support chaotic bouncing of the nucleons against each other with a wanted distribution of collision angles. Because the particles moving with high speed are stretched in direction of the moving direction it makes a difference at which angle they collide. The relativistic longitudinal-transversal mass alteration already proposed in 1899 by *Lorentz* [41] should be recast in an *IRT* compatible version then applicable to the controlled nuclear fusion, too.

A *Lattice-Boltzmann* solution is currently in progress and should be published soon. Besides the lattice-assisted part of possible cold fusion the catalyzed fusion by neutral pions π^0 should be considered. *Fukuhara* postulated that such bosons are responsible for all low-energy nuclear interactions [42].

If one speculates about the reality of a cold fusion of atomic nuclei it may ap-

propriate remembering the history of diamond synthesis, where *HPHT* synthesis has been successfully supplemented by cost-efficient *CVD* synthesis under sub-ambient conditions. In this sense the same success is desirable for cold fusion currently under progress.

6. Keeping a Watch on Nuclear Fuel Resources on Earth and Moon

This remark takes a look into the future. What would extraterrestrial powers do on earth, fight against human beings or only harvest rough materials such as deuterium from the ocean or ${}_{2}^{3}\mathrm{He}$ from the sunlit areas of the moon to fuel their spaceships, as yet unobserved but friendly? May be they already manage it. If so, we should start an across area monitoring of the sea water deuterium content to detect significant local variation before the ocean flow equalizes any left local difference. By the way, we had the technique to do this immediately, gaining also profit for other scientific areas besides precaution for the future. With respect to the deuterium extraction from seawater we can assume that an extraterrestrial power surely knows processes like the archetype *Girdler*-sulfide process (*GS* process) [43], a two-temperature isotopic exchange process, or even seawater electrolysis, or a more sophisticated rapid gas effusion process.

7. Conclusion

There is a need of applying new physics to great technological challenges of our time such as providing the world's sustainable energy needs through controlled nuclear fusion. Large investments in this technique could soon bear fruit if new relativistic corrections for mass and energy according to the *IRT* theory would be considered in computer models as well as in the equipment. Possible changes in the equipment are a task of experts, but the recalculation of energy balances of nuclear fusion reactions can also be up to cooperating readers. When exemplarily calculating the fusion probability for deuterons or protons with *Suleiman*'s *IRT* approach, one can confirm markedly different results in comparison to the non-relativistic case. The maxima of the probability shift to somewhat higher energy and the probability versus energy respectively recession speed curves are markedly broader than compared to non-relativistic calculations. Consequently, the *IRT* corrected probability results recommend to correct the existing assumptions to somewhat higher values. There exists a golden limit where already at a recession speed of $\beta = \varphi$ the fusion probability is zero. At extreme temperatures ($kT > 1$ GeV), the maximum of the fusion probability is found at $\beta = 1/3$, where baryonic matter energy and dark matter energy becomes equal. A more quantitative calculation depends on the availability of some values that should be accessed by an elaborated model calculation. The new approach should inspire researchers and big investors in the fusion technology proceed in this direction of new physics, touching besides physics the philosophical foundations of our world. The presented ideas may be extended to more cosmological questions

such as avoiding the "big bang" singularity hypothesis respectively the origin of the speed of light.

Conflicts of Interest

The author declares no conflict of interests regarding the publication of this paper.

References

[1] Suleiman, R. (2019) Relativizing Newton. Nova Scientific Publisher, New York, 1-207.

[2] Otto, H.H. (2020) Reciprocity as an Ever-Present Dual Property of Everything. *Journal of Modern Physics*, **11**, 98-121. https://doi.org/10.4236/jmp.2020.111007

[3] Otto, H.H. (2020) A Primer of Important Natural Numbers and Revisited Fundamental Physical Constants.

[4] He, J.H., Tian, D. and Otto, H.H. (2018) Is the Half-Integer Spin a First Level Approximation of the Golden Mean Hierarchy? *Results in Physics*, **11**, 362-363. https://doi.org/10.1016/j.rinp.2018.09.027

[5] Planat, M., Aschheim, R.A., Amaral, M.M., Fang, F. and Irwin, K. (2020) Complete Quantum Information in the DNA Genetic Code. *Symmetry*, **12**, 1993. https://doi.org/10.20944/preprints202007.0403.v2

[6] Clynes, T. (2020) 5 Big Ideas for Making Fusion Power a Reality. IEEE Spectrum, New York.

[7] Fukuharo, M., Yoshino, A. and Fujima, N. (2021) Earth Factories: Creation of the Elements from Nuclear Transmutation in Earth's Lower Mantle. *AIP Advances*, **11**, Article ID: 105113. https://doi.org/10.1063/5.0061584

[8] Hardy, L. (1993) Nonlocality for Two Particles without Inequalities for Almost All Entangled States. *Physical Review Letters*, **71**, 1665-1668. https://doi.org/10.1103/PhysRevLett.71.1665

[9] Suleiman, R. (2018) A Model of Dark Matter and Dark Energy Based on Relativizing Newton's Physics. *World Journal of Condensed Matter Physics*, **8**, 130-155. https://doi.org/10.4236/wjcmp.2018.83009

[10] Otto, H.H. (2020) Phase Transitions Governed by the Fifth Power of the Golden Mean and Beyond. *World Journal of Condensed Matter Physics*, **10**, 135-159. https://doi.org/10.4236/wjcmp.2020.103009

[11] Joshi, S. (2016) Theory of Quantum Relativity. *Journal of Quantum Information Science*, **6**, 249-262. https://doi.org/10.4236/jqis.2016.64016

[12] Gift, S.J.G. (2009) Separating Equivalent Space-Time Theories. *Apeiron*, **16**, 1-11.

[13] Oliphant, M.L.E., Harteck, P. and Rutherford, E. (1934) Transmutation Effects Observed with Heavy Hydrogen. *Proceedings of the Royal Society A*, **144**, 692-703. https://doi.org/10.1038/133413a0

[14] Giancarli, L. (2017) Tritium Self-Sufficiency. ITER Newsline.

[15] Iyengar, P.K. and Srinivasan, M. (1990) Overview of BARC Studies in Cold Fusion. *First Annual Conference on Cold Fusion*, Salt Lake City, 1 March 1990, 1-30.

[16] Akiba, H., Kofu, M., Kobayashi, H., Kitagawa, H., Ikeda, K., Otomo, T. and Yamamuro, O. (2016) Nanometer-Sized Effect on Hydrogen Sites in Palladium. *Journal of the American Chemical Society*, **138**, 10238-10243.

https://doi.org/10.1021/jacs.6b04970

[17] Mckubre, M. (2006) Using Resistivity to Measure H/Pd and D/Pd Loading: Method and Significance.

[18] Bhatnagar, P.L., Gross, E.P. and Krook, M. (1954) A Model for Collision Processes in Gases. *Physical Review*, **94**, 511-525. https://doi.org/10.1103/PhysRev.94.511

[19] Gamov, G. (1928) Quantum Theory of Atomic Nucleus. *Zeitschrift für Physik*, **51**, 204-212.

[20] Cooley, J. (2020) Principles of Astrophysics and Cosmology. Lecture at SMU, USA.

[21] (2019) The NIST SP 959 CODATA Recommended Values of the Fundamental Constants of Physics and Chemistry. National Institute of Standards and Technology, Gaitherburg.

[22] (2018) NIST CODATA. National Institute of Standards and Technology, Gaitherburg.

[23] Otto, H.H. (2021) Beyond a Quartic Polynomial Modeling of the DNA Double-Helix Genetic Code. *Journal of Applied Mathematics and Physics*, **9**, 2558-2577. https://doi.org/10.4236/jamp.2021.910165

[24] Otto, H.H. (2022) Golden Quartic Polynomial and Moebius-Ball Electron. 1-25.

[25] Otto, H.H. (2017) Should We Pay More Attention to the Relationship between the Golden Mean and the Archimedes' Constant? *Nonlinear Science Letters A*, **8**, 410-412.

[26] Otto, H.H. (2018) About Cauchy Functions Compared to the Gaussian Function for X-Ray Powder Diffraction Profile Fitting: An Exercise.

[27] Suleiman, R. (2021) On the Dynamics of Matter—Dark Matter Coupling: The Case of Disk Galaxies. 1-26.

[28] El Naschie, M.S. and He, J.-H. (2018) Tesla's Dream from a Modern Quantum Spacetime View Point. *Nonlinear Science Letters A*, **9**, 36-43.

[29] Otto, H.H. (2020) Magic Numbers of the Great Pyramid: A Surprising Result. *Journal of Applied Physics and Mathematics*, **8**, 2063-2071. https://doi.org/10.4236/jamp.2020.810154

[30] Otto, H.H. (2020) Ratio of In-Sphere Volume to Polyhedron Volume of the Great Pyramid Compared to Selected Convex Polyhedral Solids. *Journal of Applied Mathematics and Physics*, **9**, 41-56.

[31] Fleischmann, M. and Pons, S. (1989) Electrochemically Induced Nuclear Fusion of Deuterium. *Journal of Electroanalytical Chemistry and Interfacial Electrochemistry*, **261**, 301-308. https://doi.org/10.1016/0022-0728(89)80006-3

[32] Garai, J. (2019) Physical Model for Lattice Assisted Nuclear Reactions. 1-28.

[33] Gurbich, A.F. (2003) Physics of the Interaction of Charged Particles with Nuclei.

[34] Otto, H.H. (2016) Au Micro-Platelets: Formation and Application.

[35] Wells, P.B. (1978) The Influence on Selectivity of the Environment of Catalyst Sites: III. The Role of Hydrogen Occlusion in Group VIII Metals. *Journal of Catalysis*, **52**, 498-506. https://doi.org/10.1016/0021-9517(78)90355-X

[36] Uhm, H.S. and Lee, W.M. (1991) High Concentration of Deuterium in Palladium from Plasma ion Implantation. *Physics of Fluids B, Plasma Physics*, **3**, 3188. https://doi.org/10.1063/1.859799

[37] Flynn, H. (1982) Method of Generating Energy by Acoustically Induced Cavitation Fusion and Reactor Therefore. US Patent US4333796.

[38] Crum, A. (1998) Acoustically Induced Cavitation Fusion. *Journal of the Acoustic*

Society of America, **103**, 3012. https://doi.org/10.1121/1.422482

[39] Taleyarkhan, R., West, C., Lahey Jr., R., Nigmatulin, R. and Block, R. (2004) Additional Evidence of Nuclear Emissions during Acoustic Cavitation. *Physical Review E*, **69**, Article ID: 036109. https://doi.org/10.1103/PhysRevE.69.036109

[40] Sato, M., Sugai, H., Ishiyima, T., Holla, H., Takeidi, M. and Okada, N. (2005) Conditions of Multibubble Sonofusion and Proposal of Experimental Setup. 1-4.

[41] Lorentz, (1899) Simplified Theory of Electrical and Optical in Moving Systems. *Proceedings of the Royal Netherlands Academy of Arts and Sciences*, **1**, 427-442.

[42] Fukuhara, M. (2003) Neutral Pion-Catalyzed Fusion in Palladium Lattice. *Fusion Science and Technology*, **43**, 128-133. https://doi.org/10.13182/FST03-A254

[43] Rae, H.V. (1978) Selecting Heavy Water Processes. American Chemical Society Symposium Series, Washington DC, 1-26. https://doi.org/10.1021/bk-1978-0068.ch001

[44] Otto, H.H. (2018) Reciprocity Relation between the Mass Constituents of the Universe and Hardy's Quantum Entanglement Probability. *World Journal of Condensed Matter Physics*, **8**, 30-35. https://doi.org/10.4236/wjcmp.2018.82003

Appendix

Stability of Atomic Nuclei (Figure A1)

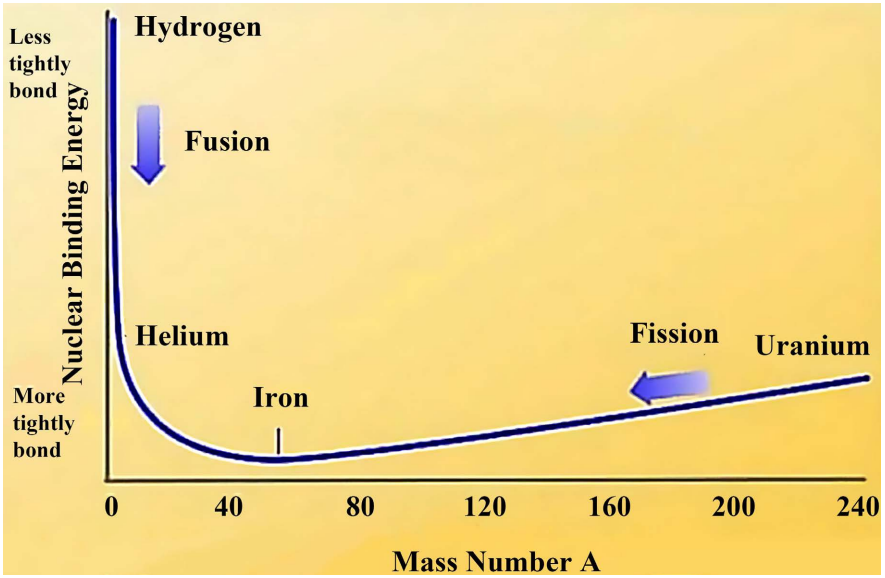

Figure A1. Sketch of the valley of stability for atomic nuclei explaining the nuclear fusion ability of elements left from the minimum (iron) respectively fission ability right from the minimum.

Maximum of the Function $f(\beta)$

The maximum of the polynomial equation as part of the integrand of Equation (23) can be found by setting the derivative equal to zero

$$f(\beta)=\frac{\beta\left(1-\beta-\beta^2\right)}{(1+\beta)\sqrt{1-\beta^2}} \tag{41}$$

$$f'(\beta)=\frac{\beta^4+\beta^3-\beta^2-3\beta+1}{(1+\beta)\left(1-\beta^2\right)^{3/2}}=0 \tag{42}$$

Result: $f_{\max}=0.147847\approx\varphi^4$ at $\beta_{\max}=0.3140262767$

Reciprocity Relation of the Function $f(\beta)$

Interestingly in the context of a previous contributions [2] [44], one can recast the function $f(\beta)$ leading to a reciprocity relation

$$f(\beta)=\frac{\beta^{3/2}}{1+\beta}\left(\sqrt{\beta^{-1}-\beta}-\left(\sqrt{\beta^{-1}-\beta}\right)^{-1}\right) \tag{43}$$

Furthermore, the zeros of the quadratic equation as part of Equation (41)

$$\beta^2-\beta+1=0 \tag{44}$$

deliver the golden mean $\beta_1=\varphi$ and its negative reciprocal $\beta_2=-\varphi^{-1}=-(\varphi+1)$ [10].

A further examination of this function yielded the following results that were depicted in Figure A2, considering the decomposition into reciprocal terms according to Equation (43). The intersection point of the basic function with the

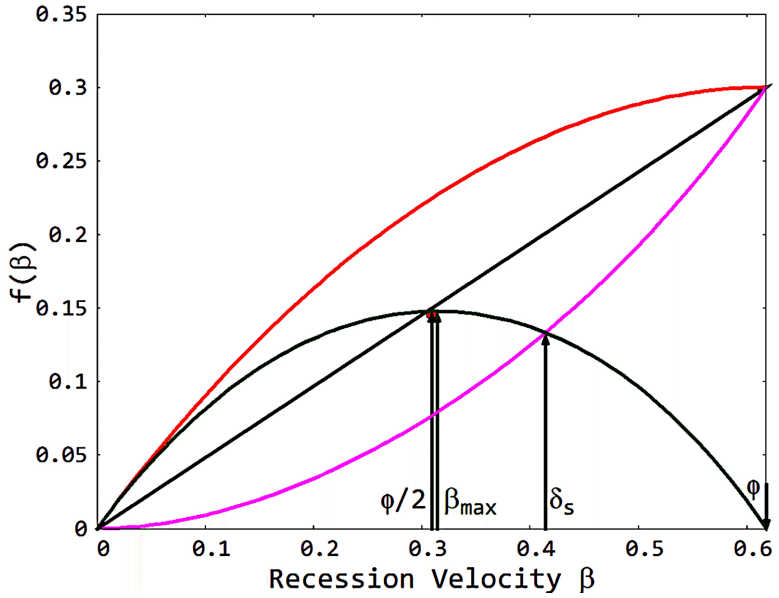

Figure A2. Illustration of the function $f(\beta)$ according to Equation (41). Green: basic function, red and magenta: decomposed reciprocal summands according to Equation (34). The red circle is located at $x=\frac{\varphi}{2}, y=\varphi^4$.

magenta curve at $\varphi=\sqrt{2}-1=0.41421356\cdots$ is remarkable. The result representing the silver mean is given by solving the quadratic equation

$$\beta^2+2\beta-1=0 \tag{45}$$

giving zeros at $\beta_3=\sqrt{2}-1$ respectively $\beta_4=-\left(\sqrt{2}+1\right)$.

Furthermore interesting is the value of $\sqrt{\beta^{-1}-\beta}$ at $\beta=\varphi/2$ yielding

$$\sqrt{\frac{2}{\varphi}-\frac{\varphi}{2}}=1.710862\cdots\approx\frac{\ln(2)}{\ln(3)-\ln(2)}=1.709511\cdots \tag{46}$$

This numerical similarity may be important when interpreting *Suleiman*'s result for rotating galaxies. When relating the galaxy's scale radius r_s, at which the rotation velocity equals half of its maximum value, to the galactic core radius r_c, where the energy densities of matter and dark matter are predicted to be equal [1], then one is faced exactly with the value $\frac{r_s}{r_c}=1.70951$ [27].

$\beta_{\max}$ respectively E values put in brackets were calculated for the non-relativistic case according to Equation (23). The maximum of $\langle\sigma\beta\rangle/S_0$ is given in different color (**Table A1**).

Table A1. *IRT*-corrected deuteron fusion data for selected values of kT.

kT (keV)	$\beta_{\max}$	$\Delta\beta_{\max}$	$\Delta\beta_{\max}/\beta_{\max}$	E (keV)	$\langle\sigma\beta\rangle_{\max}/S_0$
10000	0.130213 (0.07878)	0.20244	1.5547	6118.5 (2910.1)	0.058405
8617	0.121788 (0.074967)	0.18575	1.5252	5444.8 (2635.2)	0.06656
2000	0.064038 (0.046070)	0.07773	1.2137	1691.4 (995.2)	0.2037

Continued

1000	0.047875 (0.036566)	0.05261	1.0989	976.5 (627.0)	0.3069
500	0.036135 (0.029022)	0.03593	0.9943	569.8 (395.0)	0.4179
200	0.025238 (0.021384)	0.02196	0.8701	284.0 (214.4)	0.51504
160.4	**0.023188 (0.019868)**	**0.01953**	**0.8422**	**240.7 (185.1)**	**0.5197**
100	0.019375 (0.016972)	0.01518	0.7832	168.8 (135.1)	0.4983
50	0.014985 (0.013471)	0.01054	0.7033	102.2 (85.1)	0.38616
20	0.010750 (0.009925)	0.00659	0.6133	53.0 (46.2)	0.18011
17.2347	0.01019 (0.009445)	0.00610	0.5988	47.7 (41.8)	0.15046
10	0.00840 (0.007878)	0.00465	0.5536	32.5 (29.1)	0.0664
8.6173	0.007965 (0.007497)	0.004276	0.5368	29.3 (26.4)	0.0507
1	0.003765 (0.003657)	0.001425	0.3785	6.63 (6.27)	4.05×10^{-5}
0.1	0.001720 (0.001697)	0.000458	0.2660	1.39 (1.35)	2.198×10^{-13}
0.01	0.0007925 (0.0007878)	0.000140	0.1767	0.294 (0.291)	1.552×10^{-32}

Values of the relative width $\Delta\beta_{max}/\beta_{max}$ that differ by a power of ten in temperature can be scaled by ln(2) division. In this way further values can be generated as given in Table A2 in brown color. In the same way one can scale down consecutive values of β_{max} by $\pi - 1 = 2.16159$ division respectively $\Delta\beta_{max}$ by $\pi = 3.14159$ division because $\frac{\pi-1}{\pi} = 0.68169 \approx \ln(2) = 0.69315$.

Table A2. Full-width of fusion probability curves at "Low" temperature comparing deuterons with protons.

T(K)	Deuterons			Protons		
	β_{max}	$\Delta\beta_{max}$	$\Delta\beta_{max}/\beta_{max}$	β_{max}	$\Delta\beta_{max}$	$\Delta\beta_{max}/\beta_{max}$
10^6	0.0016143	0.0004084	0.2489			
10^5	0.0007538	0.0001300	0.1725	0.0009423	0.0001315	0.1912
10^4	0.0003485	0.0000414	0.1188	0.0004400	0.0000583	0.1325
10^3	0.0001617	0.0000131	0.0812	0.0002038	0.0000184	0.0903
5×10^2				0.0001617	0.0000129	0.0800

Fundamental Constants and Quantities (Table A3)

Table A3. Used fundamental constants and quantities [3] [21] [22].

Notation	Symbol	Quantity	Unit
Speed of light	c	2.99792458×10^8	m/s
Boltzmann constant	k	$8.617333262 \times 10^{-11}$	MeV·K^{-1}
Avogadro number	N_A	$6.02214076 \times 10^{23}$	mol^{-1}
Sommerfeld constant	A	$7.2973525693(11) \times 10^{-3}$	-

Continued

Proton rest energy	${}_{1}^{1}\mathrm{H}$	938.27208816(29)	MeV
Deuteron rest energy	${}_{1}^{2}\mathrm{D}$	1875.61294257(57)	MeV
Golden mean	$\varphi = \frac{\sqrt{5}-1}{2}$	0.61803398874…	-
Silver mean	$\sqrt{2}-1$	0.41421356237…	-